



Tilted Circumbinary Planetary Systems as Efficient Progenitors of Free-floating Planets

Cheng Chen¹, Rebecca G. Martin^{2,3}, Stephen H. Lubow⁴, and C. J. Nixon¹¹ School of Physics and Astronomy, University of Leeds, Sir William Henry Bragg Building, Woodhouse Lane, Leeds LS2 9JT, UK² Department of Physics and Astronomy, University of Nevada, Las Vegas, 4505 South Maryland Parkway, Las Vegas, NV 89154, USA³ Nevada Center for Astrophysics, University of Nevada, Las Vegas, 4505 South Maryland Parkway, Las Vegas, NV 89154, USA⁴ Space Telescope Science Institute, 3700 San Martin Drive, Baltimore, MD 21218, USA

Received 2023 October 20; revised 2023 December 18; accepted 2023 December 21; published 2024 January 11

Abstract

The dominant mechanism for generating free-floating planets has so far remained elusive. One suggested mechanism is that planets are ejected from planetary systems due to planet–planet interactions. Instability around a single star requires a very compactly spaced planetary system. We find that around binary star systems instability can occur even with widely separated planets that are on tilted orbits relative to the binary orbit due to combined effects of planet–binary and planet–planet interactions, especially if the binary is on an eccentric orbit. We investigate the orbital stability of planetary systems with various planet masses and architectures. We find that the stability of the system depends upon the mass of the highest-mass planet. The order of the planets in the system does not significantly affect stability, but, generally, the most massive planet remains stable and the lower-mass planets are ejected. The minimum planet mass required to trigger the instability is about that of Neptune for a circular orbit binary and a super-Earth of about 10 Earth masses for highly eccentric binaries. Hence, we suggest that planet formation around inclined binaries can be an efficient formation mechanism for free-floating planets. While most observed free-floating planets are giant planets, we predict that there should be more low-mass free-floating planets that are as of yet unobserved than higher-mass planets.

Unified Astronomy Thesaurus concepts: [Exoplanet dynamics \(490\)](#); [Exoplanet systems \(484\)](#); [Three-body problem \(1695\)](#); [N-body simulations \(1083\)](#); [Computational astronomy \(293\)](#); [Binary stars \(154\)](#)

1. Introduction

Gravitational microlensing observations suggest that there could be a significant population of free-floating planets (FFPs; e.g., Sumi et al. 2011; Clanton & Gaudi 2017). Estimates for the mass of FFPs range from around 0.25 (M_{J}) (Mróz et al. 2017) up to about 3.5 (Sumi et al. 2011) Jupiter masses per main-sequence star. More recently, the MOA-II 9 yr Survey toward the Galactic Bulge found an average of 0.54 M_{J} of FFP per main-sequence star (Koshimoto et al. 2023; Sumi et al. 2023). Based on the lower end of these estimates, there is an excess of FFPs by a factor of up to 7 compared to that predicted by core-collapse models (Miret-Roig et al. 2021). There are several mechanisms suggested to form the excess of FFPs. These include planet–planet scattering (Rasio & Ford 1996; Weidenschilling & Marzari 1996; Veras & Raymond 2012), aborted stellar embryo ejection from a stellar nursery (Reipurth & Clarke 2001), and photoerosion of a prestellar core by stellar winds from a nearby OB star (Whitworth & Zinnecker 2004). Planet–planet scattering around single stars cannot explain the large number of FFPs (Veras & Raymond 2012; Ma et al. 2016).

Planetary system instability around a single star or a coplanar binary occurs only when the planets are compactly spaced (see Section 2.1 for more details). While most studies of circumbinary planet (CBP) stability have assumed the coplanarity of the planetary system to the binary orbit, the stability of CBPs is also affected by the inclination of the planet orbit relative to the binary orbit (Doolin & Blundell 2011; Chen

et al. 2020). Even widely spaced planetary systems can be unstable around a tilted binary (see Section 2.2). Thus the ejection of planets from a misaligned binary system can be far more efficient compared to a single star or coplanar binary system (see also Childs & Martin 2022).

The current known population of CBPs are all in near-coplanar configurations (e.g., Orosz et al. 2012a; Welsh et al. 2012; Kostov et al. 2013; Standing et al. 2023). Recently several multi-CBP systems have been discovered. For example, (i) Kepler-47 has three planets with masses of 2.07, 19.02, and 3.17 M_{\oplus} CBPs (Orosz et al. 2012a, 2012b; Kostov et al. 2013); (ii) TOI-1338 hosts two CBPs with masses of 33 and 65 M_{\oplus} ; (iii) NN Ser has two Jupiter-mass CBPs with masses of 2.28 and 6.91 M_{J} (Kostov et al. 2020; Standing et al. 2023); and (iv) Kepler-451 has three Jupiter-mass CBPs with masses of 1.76, 1.86, and 1.61 M_{J} (Baran et al. 2015; Esmer et al. 2022). These observational results suggest that multiplanet circumbinary systems may not be rare, and this is consistent with the Kepler data for planets around single stars that show that at least around half of planets have siblings (e.g., Berger et al. 2018; Thompson et al. 2018). While the observed population of CBPs is nearly coplanar, it is acknowledged that the lack of inclined CBPs is likely to be a selection effect (e.g., Martin & Fabrycky 2021). In particular, inclined planetary systems may be expected around binaries with longer orbital periods (Czekala et al. 2019). Such inclined CBP systems may be observed in the future with eclipse-timing variations (Martin 2019; Zhang & Fabrycky 2019).

Observations of circumbinary disks, the birthplace for these planets, suggest that a large inclination between the binary orbital plane and the disk may be common (e.g., Chiang & Murray-Clay 2004; Winn et al. 2004; Capelo et al. 2012; Brinch et al. 2016; Zhu et al. 2022). Polar aligned disks around

eccentric binaries may also be common (Kennedy et al. 2012, 2019; Kenworthy et al. 2022). Chaotic accretion can lead to the formation of inclined circumbinary disks (Clarke & Pringle 1993; Bate 2018) and subsequent disk evolution can lead to tilt evolution toward a coplanar alignment (Papaloizou & Terquem 1995; Bate et al. 2000; Lubow & Ogilvie 2000; Nixon et al. 2011) or a polar alignment (Aly et al. 2015; Martin & Lubow 2017; Zanazzi & Lai 2017; Lubow & Martin 2018). However, the alignment timescale for an extended disk may be longer than the disk lifetime and planetary systems may form in a inclined disk.

In this Letter, we consider the stability of tilted planetary systems with unequal-mass planets. We show that the planet with the highest mass dominates the stability outcome. The order of the orbital radii of the planets does not change the stability; ejection of the smaller mass planets is the most likely outcome. We examine the planet mass required for planet–planet interactions to drive instability. We discuss the planetary system stability in Section 2, and we describe our simulation setup and parameter domains we explore in Section 3. Specifically, we consider the masses of the ejected planets. We show our simulation results in Section 4. Finally, a discussion and conclusions follow in Sections 5 and 6.

2. Planetary System Stability

In this section we describe the instability mechanisms for coplanar and tilted CBP systems.

2.1. Coplanar Circumbinary Planets

Around a single star, planet–planet scattering occurs when the planets form close to each other. Two planets with masses m_{p1} and m_{p2} that form with semimajor axes a_{p1} and a_{p2} , respectively, around a star with mass m are unstable if $\Delta = (a_{p2} - a_{p1})/R_{\text{Hill}} \lesssim 2\sqrt{3}$ (Marchal & Bozis 1982; Gladman 1993; Chambers et al. 1996), where the mutual Hill sphere radius is given by

$$R_{\text{Hill}} = \left(\frac{m_{p1} + m_{p2}}{3m} \right)^{1/3} \left(\frac{a_{p1} + a_{p2}}{2} \right). \quad (1)$$

Ejection of giant planets in simulations of planet formation around a single star is unlikely and most ejected planets have a mass $\lesssim 0.3 M_{\oplus}$ (Barclay et al. 2017). This stability criterion is not significantly affected if a single star is replaced by a *coplanar* inner binary, unless the planets are formed very close to the binary (Kratte & Shannon 2014). The minimum radius of a stable orbit of a coplanar CBP was studied by Holman & Wiegert (1999), who developed empirical expressions involving the binary eccentricity and the binary mass fraction. However, the outcome of an unstable system is more likely to be ejection rather than a collision around a binary star system because of close encounters with the binary (Smullen et al. 2016; Sutherland & Fabrycky 2016; Gong & Ji 2017; Gong 2017; Fleming et al. 2018). Coplanar planets around a binary must form relatively close to each other for the system to be unstable. Smullen et al. (2016) investigated the orbital stability of multi-CBP systems for low inclination ($i < 6^\circ$). They pointed out that the average loss rate for planets is very similar between planets around a binary and a single star and so they concluded that the orbital stability has a weak dependence

on how compact the initial semimajor axis distribution is for planets around a binary or a single star. In contrast, Chen et al. (2023a) considered two tilted CBPs and found wide instability even in cases where planets are very widely spaced.

2.2. Tilted Circumbinary Planets

Contrary to coplanar CBP systems, a multiplanet system with orbits that are tilted with respect to the inner binary can be unstable for a wide range of initial planet separations (Chen et al. 2023a, 2023b). A planet orbiting around an eccentric binary undergoes tilt oscillations as a result of its interaction with the binary, which is the nodal oscillation (Verrier & Evans 2009; Farago & Laskar 2010; Naoz et al. 2017; Chen et al. 2019). Planets in a tilted two-CBP system also undergo mutual tilt oscillations as a result of planet–planet interactions. Their longitude of ascending nodes may be locked or unlocked relative to each other depending upon their spacing (Chen et al. 2022). If the mutual inclination between the two CBPs becomes large due to the complicated results of these interactions, the outer planet can induce von Zeipel–Kozai–Lidov (ZKL; von Zeipel 1910; Kozai 1962; Lidov 1962) oscillations of the inner planet leading to eccentricity growth of the planet’s orbit. The mutual inclination Δi_p between the two planets is given by

$$\Delta i_p = \cos^{-1}(\hat{l}_{p1} \cdot \hat{l}_{p2}), \quad (2)$$

where \hat{l}_{pi} for $i = 1, 2$ is a unit vector in the direction of the angular momentum of each planet. Figures 4 and 7 in Chen et al. (2023a) demonstrate that inclined CBPs can undergo eccentricity oscillations that may be due to the octupolar forcing of the eccentric binary (the outer particle Lidov–Kozai mechanism; Naoz et al. 2017) or due to planet–planet interactions, or a combination of both.

Initially, the mutual inclination between the two CBPs is 0° but it oscillates over time because they have the different nodal precession rates and undergo mutual tilt oscillations. Mean motion resonances (MMRs) between the planets are typically stable in a coplanar configuration, but they become unstable in a tilted planetary system. Therefore, the complex dynamics around a tilted binary can lead to instability for a wide range of initial planet semimajor axes (Chen et al. 2023a).

3. Simulation Setup and Parameter Space Explored

To study the orbital stability of planetary systems with unequal-mass planets we carry out simulations with the n -body package, REBOUND, with a WHFAST integrator that is a second-order symplectic Wisdom Holman integrator with 11th-order symplectic correctors (Rein & Tamayo 2015). We choose a fixed time step that is 0.05 times the binary orbit. WHFAST solves equations of the motion with the Hamiltonian splitting in the Jacobi coordinates that are measured relative to the center of mass of all bodies (see Rein & Tamayo 2015 for further details). The central binary has components of masses m_1 and m_2 with a total mass $m_1 + m_2 = m_b$. We consider an equal-mass binary with $m_1 = m_2 = 0.5 m_b$ so that the mass fraction of the binary $f_b = 0.5$. We simulate binaries with both a circular and an eccentric orbit where the binary eccentricity is e_b and the binary semimajor axis is a_b .

We consider planetary systems with two planets. We explored the extension to three-planet systems in Chen et al.

Table 1
Parameters of the Simulations

Model	e_b	$m_{p1} (m_b)$	$m_{p2} (m_b)$
A1	0.0	0.000003	0.001
A2	0.8	0.000003	0.001
C1	0.0	0.001	0.000003
C2	0.8	0.001	0.000003
E1	0.0	0.000003	0.000003
E2	0.8	0.000003	0.000003
SE1	0.0	0.00003	0.00003
SE2	0.8	0.00003	0.00003
N1	0.0	0.00005	0.00005
N2	0.8	0.00005	0.00005
S1	0.0	0.0003	0.0003
S2	0.8	0.0003	0.0003

Note. The first column contains the name of model; the second, third, and fourth columns indicate the binary eccentricity and the masses of inner and outer planets.

(2023b), where we found that the instability in the three-planet case is qualitatively similar to the two-planet case when the three planets are separated by a fixed number of mutual Hill radii. Three-planet systems are slightly more unstable than two-planet systems. The number of planets that are ejected in unstable systems depends upon how close the system is to the binary. Close-in systems are more likely to eject more planets. The planetary system arrangements for each simulation are shown in Table 1.

The two planets are initially on Keplerian orbits around the center of mass of the binary. Their orbits are defined by six orbital elements: the semimajor axes a_{p1} and a_{p2} , inclinations i_{p1} and i_{p2} that are relative to the binary orbital plane, eccentricities e_{p1} and e_{p2} , longitudes of the ascending nodes ϕ_{p1} and ϕ_{p2} measured from the binary semimajor axis, arguments of periapsides ω_{p1} and ω_{p2} , and true anomalies ν_{p1} and ν_{p2} . The initial orbits of the two planets are coplanar to each other and circular, so initially $e_p = 0$, $\omega_p = 0$, and $\nu_p = 0$, and we set $\phi_p = 90^\circ$ for all planets. We integrate the simulations for a total time of 14 million binary orbital periods (T_b).

We describe the criteria for determining an unstable orbit of the planet based on three distinct conditions. First, if the eccentricity of the planet's orbit $e_p \geq 1.0$, the planet is deemed unbound from the binary system. Second, an orbit is unstable if the semimajor axis of the planet's orbit $a_p > 1000 a_b$, indicating that the planet has moved excessively far away from the central system. Third, if the semimajor axis of the planet's orbit becomes smaller than that of the binary's orbit, $a_p < a_b$, the planet can no longer be considered a CBP. To prevent unwanted numerical errors, we remove the mass of the unstable CBP when it is far enough from the central binary. These stability criteria are established in line with existing research (e.g., Chen et al. 2020; Quarles et al. 2020; Chen et al. 2023a, 2023b).

To understand the dynamical interaction between two planets, the inner planet is placed at $a_{p1} = 5 a_b$, where it should be stable for a single CBP (Chen et al. 2020). We vary the semimajor axis of the outer planet by varying the ratio of their mutual Hill radius between the inner planet, Δ , and thus

we have

$$a_{p2} = a_{p1} + \Delta \left(\frac{m_{p1} + m_{p2}}{3 m_b} \right)^{1/3} \left(\frac{a_{p1} + a_{p2}}{2} \right), \quad (3)$$

and Δ ranges from 3.4 ($\approx 2\sqrt{3}$) to 12.0 with an interval of $\Delta = 0.1$.

4. Simulation Results

In this section we describe the results of our simulations. We consider (i) the effect of having an unequal-mass planetary system, (ii) the radial order of the planets from the binary, and (iii) the planet mass required for instability.

4.1. The Effect of Unequal-mass Planetary Systems

Figure 1 shows stability maps in which the x -axis is the initial inclination i_p of two CBPs with respect to the binary with an interval of 2.5° and the y -axis is the initial separation between two planets in units of R_{Hill} . The colors of the pixels show the planets' orbital status at the end of simulations. The blue pixels represent systems in which the two planets are stable. The red pixels represent systems in which only the outer planet is stable, and the green pixels represent systems in which only the inner planet is stable. White pixels represent systems in which the two planets are unstable. The cyan, orange, and pink horizontal dashed lines indicate the 2:1, 5:2, and 3:1 MMRs between the two planets. Note that the location of the MMRs are shifted relative to Δ compared to the equal Jupiter-mass planet cases in Chen et al. (2023b). The total mass of the two CBPs in this study is smaller than two Jupiter-mass CBPs, so their separation in terms of R_{Hill} is smaller for a fixed Δ .

The top panels of Figure 1 show stability maps for models A1 and A2 that are planetary systems with an inner Earth-mass planet and an outer Jupiter-mass planet with binary eccentricity $e_b = 0.0$ (left) and 0.8 (right). In model A1 with a circular orbit binary, if the two planets are near aligned to the binary orbital plane (in prograde or retrograde orbits), they can be stable even if they have very small separation ($\Delta \geq 3.5$). However, with higher inclination orbits, the two planets are unlikely to be stable until $\Delta \geq 5.0$. Above this region, there are unstable regions around the 2:1 and 3:1 MMRs. The effect of the 5:2 MMR is minor and there are sporadic unstable orbits around it. The only unstable outcome for a system with an inner Earth-mass and an outer Jupiter-mass planet is that the Earth-mass planet gets ejected.

For model A2 with an eccentric binary, there are more inner planet unstable orbits within $\Delta \leq 5.0$ showing that inclined planets are not likely to be stable within the 2:1 MMR region except around the polar orbit (i_p around 90°). All of the unstable cases are the outer planet stable cases meaning that the inner Earth-mass planet is ejected. Moreover, the unstable regions around 2:1 and 3:1 MMRs become larger than those of model A1. Two planets are unlikely to be stable even when they are just slightly inclined to the binary. We also increased the mass of the inner planet to 1 Saturn mass and found most of the unstable cases again involve the ejection of the lower-mass inner planet.

These two panels can be compared with the top left and bottom right panels of Figure 2 in Chen et al. (2023a), which show the same maps but for two Jupiter-mass CBPs. The units of the y -axis are different, but otherwise the stability map is very similar, except that in the unequal-mass system shown

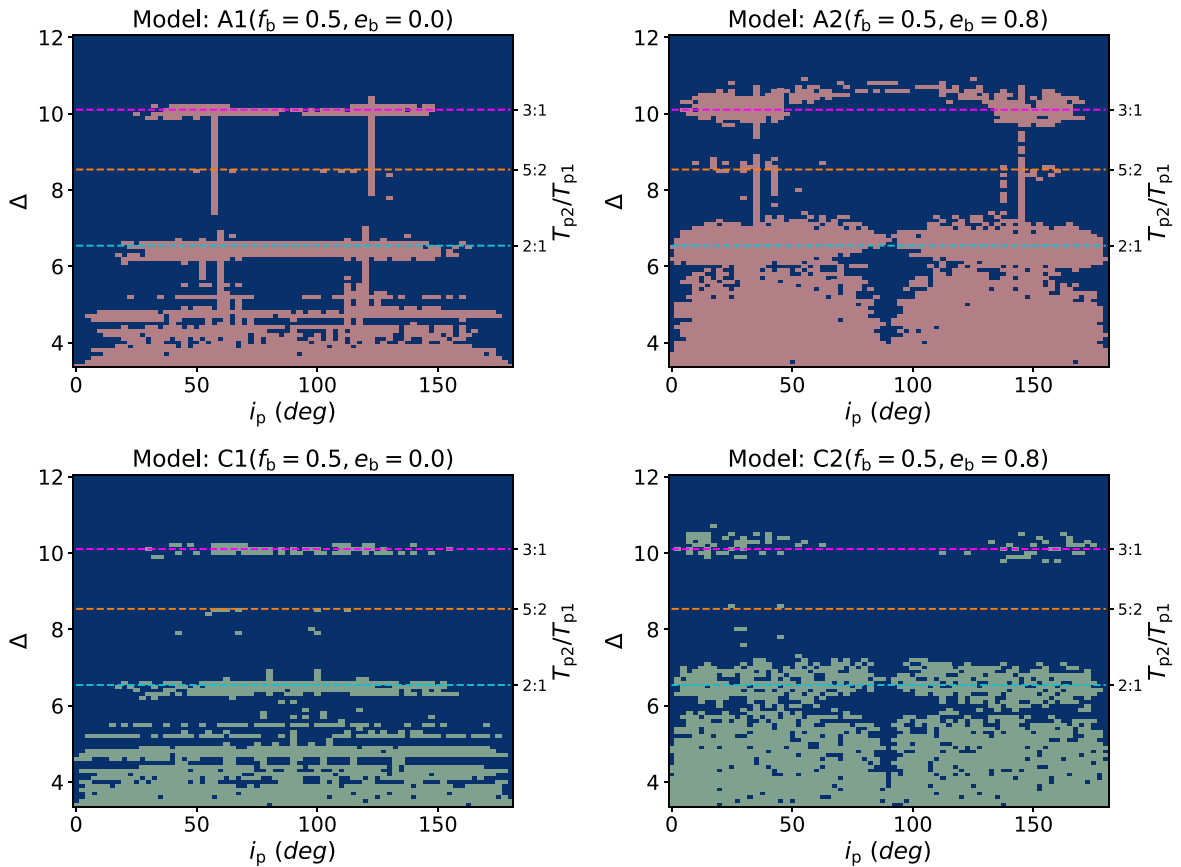


Figure 1. Stability maps of a two-planet circumbinary system with $e_b = 0.0$ (left panels) and 0.8 (right panels). The planetary system consists of one Earth-mass planet and one Jupiter-mass planet. The Jupiter-mass planet is the outer planet in the top panels and is the inner planet in the bottom panels. The inner planet has initial semimajor axis $a_{p1} = 5 a_b$, and the y -axis is Δ with an interval of 0.1 , while the x -axis is the initial inclination of two planets with an interval of 2° . The four horizontal dashed lines represent the 2:1 (cyan), 5:2 (orange), 3:1 (pink), and 4:1 (red) MMRs between the two planets. The four different colors of pixels represent two-planet stable cases (blue), the inner planet survived cases (green), the outer planet survived cases (red), and both planet unstable cases (white).

here, only the outer (and more massive) planet survives in all unstable cases. The two Jupiter-mass CBP systems have a small fraction of systems in which both planets are ejected; however, with the Earth-mass planet here, there are no systems in which both planets become ejected. Given the similarity between stability maps with two Jupiter-mass planets and one Jupiter and one Earth, this suggests that the mass of the most massive planet in the system is what determines the stability of the system.

4.2. The Effect of the Planetary System Order

We now change the orbital arrangement of the two planets. The bottom panels of Figure 1 show models C1 and C2 that have the same setup as models A1 and A2, except the inner planet is the Jupiter-mass planet and the outer planet is the Earth-mass planet. The stability map is not significantly affected by changing the order of the planets. However, the outer massive CBPs can destabilize wider regions around the MMRs with an inner massive CBP. The lower-mass planet is ejected no matter where it begins and the Jupiter-mass planet remains stable. The system is slightly more stable with the Jupiter-mass planet being the inner planet. This is because an Earth-mass planet that is interior to the more massive outer planet is more likely to undergo secular eccentricity oscillations as their mutual inclination has increased due to the different nodal oscillation rates and they undergo tilt oscillations. This results in an increased eccentricity, interaction with the binary,

and (when the planet gets sufficiently close to the binary) subsequent ejection.

4.3. The Minimum Mass to Drive the Instability

Now we consider the minimum mass of the planet required to drive instability through planet–planet interactions. If the effect of planet–planet interactions is small, each CBP only interacts with the binary so then their orbital stability should comply with the three-body stability map (e.g., Doolin & Blundell 2011; Quarles et al. 2018; Chen et al. 2020). We have shown that the most massive planet in the system dominates the stability already so we now consider systems of equal masses but we vary the mass. We consider two CBPs of Earth mass (models E1 and E2), 10 Earth mass (models SE1 and SE2), Neptune mass (models N1 and N2), and Saturn mass (models S1 and S2).

The left panels of Figure 2 show the effect of increasing the planet masses around a circular orbit binary. Two Earth-mass CBPs (model E1) are very stable. With increasing masses of two planets, the number of unstable cases increases. For model S1 in which the planets are Saturn mass, the stability map is very similar to the map of A1 in Figure 1 with Jupiter-mass planets. Around a circular orbit binary, instability requires a planet mass greater than about Neptune’s mass to drive planetary system instability.

The right panels of Figure 2 show the same simulations with increasing planet masses but around an eccentric orbit binary

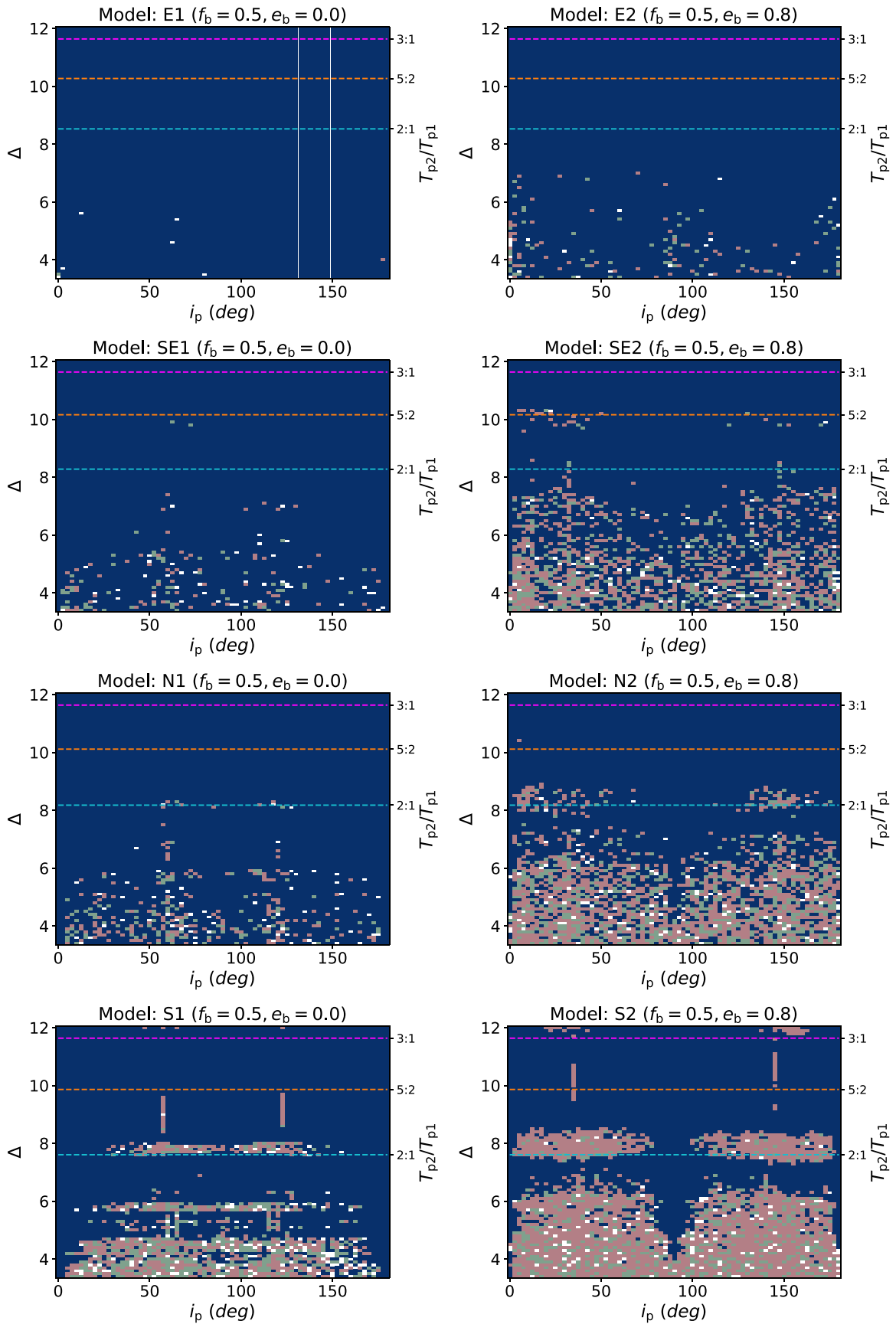


Figure 2. Stability maps for planetary systems with two equal-mass circumbinary planets around a binary system with $e_b = 0.0$ (left panels) and 0.8 (right panels). The inner planet has initial semimajor axis $a_{p1} = 5 a_b$. The pixel colors are as described in Figure 1. From top to bottom panels, the two planets are Earth mass, super-Earth mass (10 times Earth mass), Neptune mass, and Saturn mass.

with $e_b = 0.8$. The Earth-mass planets are still stable, but there are some unstable cases at separations closer than the 2:1 MMR. For the super-Earth-mass planets, more than half of the pixels are unstable for separations closer than the 2:1 MMR in models SE2 and N2. For model S2, with Saturn-mass planets, the map is very similar to that for A2 in Figure 1, and two planets can only be stable in near-coplanar or polar orbits within the 2:1 MMR. Around a highly eccentric orbit binary, instability requires lower-mass planets than those around circular orbit binaries. Planet–planet interactions drive instability for planet masses greater than super-Earth masses for these cases (which have $a_{p1} = 5a_b$).

5. Discussion

Planet–planet scattering, gravitational instabilities in the outer disk, and post-formation evolution around single-star systems may contribute some population of the observed FFPs, but it is difficult to explain the large populations that we have observed (Boss 2011; Veras & Raymond 2012). Recently, some N -body simulations have confirmed this point. For example, simulations with Jupiter- and Saturn-mass planets around a solar-type star show that approximately one-third of the initial disk mass is ejected (~ 5 Earth mass) in the late stage of planet formation, but the masses of the individual ejected bodies are $\lesssim 0.3$ Earth mass (Barclay et al. 2017). Pfyffer et al. (2015) found that the median mass of an ejected planet is ≤ 2 Earth mass from post-formation evolution. We also investigated multiplanetary single-star systems with two Jupiter-mass planets and found that they are very stable unless they are extremely compactly spaced with $\Delta \leq 2.3$ (see Figure 1 of Chen et al. 2023a). Thus it is difficult to find an efficient route for ejecting planets from single-star systems, particularly for large planet masses.

On the other hand, binary stars are common in the Universe, with about 40%–60% of M to F stars found to be in binary systems (Raghavan et al. 2010). Approximately half of these binaries have separations of less than 20 au, indicating that they may have circumbinary disks (CBDs) during their formation (see Figures 12 and 13 in Raghavan et al. 2010). The distribution of binary eccentricities is also broad (see Figure 14 in Raghavan et al. 2010). Further, CBDs have a wide distribution of inclinations if the binary period $T_b > 30$ days (Czekala et al. 2019). Therefore, if CBP formation occurs while the disk is young, it is likely that multiple CBPs can form within the disk. These planets can either decouple from the disk (e.g., Martin et al. 2016; Franchini et al. 2020) and be ejected or be ejected once the disk has dispersed (see Turrini et al. 2020). Therefore, while inclined CBP systems around eccentric binaries may be a common initial condition, these systems are likely to be dynamically unstable. Inclined multi-CBP systems are only likely to remain stable if the planet masses are low enough.

According to our simulations, a binary with a lower eccentricity has a higher chance to host a compact CBP pair while only a compact Earth-mass CBP pair could be stable around a binary with high eccentricity. Consequently, FFPs ranging from low to high mass can be generated from the CBP systems. Moreover, recent observations show that 93% of exoplanet pairs are at least $10 R_{\text{Hill}}$ apart (Weiss et al. 2018) and CBPs pairs may have a similar distribution due to instabilities within the 3:1 MMR.

In all of our simulations we have chosen the inner planet semimajor axis to be $a_{p1} = 5.0a_b$ since this is close to the inner stability limit for inclined orbits of all inclinations. According to Figures 3 and 5 in Chen et al. (2023a), the instabilities are stronger for inclined CBPs if the inner planet is at 10.0 or 20.0 a_b due to the secular eccentricity oscillations. However, if the inner planet is much farther from the binary, then the system behaves as though the binary is a single star. The only instability is then due to planet–planet interactions and the system becomes more stable.

6. Summary and Conclusions

In this study, we explored the stability of a pair of CBPs with varying binary eccentricity, varying planetary orbital inclination, varying planet masses, and varying planetary spacing. For the simulations presented here we took the binary to be equal mass, and the inner planet’s semimajor axis to be initially 5 times the binary semimajor axis. This case is known to be quite stable against planet–binary interactions when there is only a single planet (Chen et al. 2020). For inclined planetary orbits, especially around an eccentric binary and with higher-mass planets present in the system, we find that introducing a second planet leads to widespread instability resulting in the ejection of one or both planets.

We first considered cases with unequal-mass planets including a Jupiter-mass and an Earth-mass planet. Comparing with previous stability maps with two Jupiter-mass planets (Figure 2 of Chen et al. 2023a), we find that the stability maps with different mass planets are slightly more stable, but are qualitatively very similar. However, here we find that only the more massive Jupiter-mass planet can survive in the unstable cases. Thus, a Jupiter-mass planet tends to kick out other low-mass CBPs if they are in initially inclined orbits with respect to the binary. The ordering of the planets does not play a significant role, but a low-mass CBP can be slightly more stable if it is located outside of a massive CBP.

We examined the dependence of the orbital instability on planet mass by considering CBP systems with equal-mass planets for several values of planet mass and two values of binary eccentricity. We find that the unstable regions generally expand with increasing planet mass and with increasing binary eccentricity. We find that CBPs with $m_p \gtrsim$ Neptune mass around a circular or eccentric orbit binary are unstable, while CBPs with each planet having mass $m_p \gtrsim 10$ Earth mass are unstable around an eccentric binary. Two CBPs with $m_p \geq$ Saturn mass have a similar stability as two Jupiter-mass planets. Consequently, we may find that compact planetary systems are more stable when the binary eccentricity e_b is low. We note that our simulations are scale free so that the minimum planet mass required to trigger instability can vary with the total mass of the binary.

Our results imply that

1. Systems that initially contain multiple inclined CBPs with a range of masses will likely be unstable once the gas disk has dissipated, resulting in the ejection of the lower-mass planets independent of their radial ordering;
2. High-mass inclined CBPs can also be ejected efficiently in systems where there are multiple high-mass CBPs, and this additional constraint implies that there should be a smaller number of high-mass ejections;

3. And that inclined CBP systems are likely composed of either one high-mass planet (with any other planets at large radial separations) or several low-mass planets (occurring in systems where a high-mass planet was not present to cause instability).

These findings have important implications for the population of FFPs. In particular, if instability in inclined CBP systems is a dominant mode of FFP production, then we can expect that there are significantly more low-mass FFPs than high-mass ones. Current findings suggesting a total ejection mass of FFPs at 0.25 or 0.54 M_J per star (Mróz et al. 2017; Koshimoto et al. 2023; Sumi et al. 2023), and in the next few years the Nancy Grace Roman Space Telescope is expected to find FFPs with masses down to that of Mars and is anticipated to detect ~ 1000 FFPs, including hundreds with masses ranging from 0.1 to 1.0 M_{\oplus} (Sumi et al. 2023). We have suggested here that these FFPs may be generated by instability in inclined multi-CBP systems, as these systems are inherently more unstable than either aligned CBP systems or multiplanet systems around single stars.


To determine the fraction of FFPs produced by these different production mechanisms requires a population synthesis modeling that includes several parameters that are currently poorly constrained, including the efficiency of planet formation in circumbinary disks compared to circumsingle disks and the inclination distribution of circumbinary disks at the point at which planets decouple from their natal gas disks. However, given that (i) the broad range of inclinations observed for CBDs (Czekala et al. 2019); (ii) the realization that planet formation is a highly efficient process that begins early in the star-forming phase (Manara et al. 2018; Nixon et al. 2018; Tychoniec et al. 2020), implying that planet formation in CBDs is likely to be as efficient as planet formation around single stars; and (iii) binaries represent a significant fraction of stellar systems, we argue that it seems reasonable that instability in such systems may be the dominant mode of generating FFPs. As our understanding of the planet formation process improves we hope to address this question quantitatively in the future with detailed population synthesis models.

Acknowledgments

We thank the anonymous referee for a thorough reading of the manuscript and constructive comments that helped improve the manuscript. Computer support was provided by UNLV's National Supercomputing Center and the DiRAC Data Intensive service at Leicester, operated by the University of Leicester IT Services, which forms part of the STFC DiRAC HPC Facility (<https://dirac.ac.uk/>). C.C. and C.J.N. acknowledge support from the Science and Technology Facilities Council (grant number ST/Y000544/1). C.C. thanks Dr. Wei Zhu for the useful discussion at the PPVII conference. R.G.M. and S.H.L. acknowledge support from NASA through grants 80NSSC19K0443 and 80NSSC21K0395. C.J.N. acknowledges support from the Leverhulme Trust (grant number RPG-2021-380). Simulations in this Letter made use of the REBOUND code (Rein & Liu 2012) with the WHFAST integrator (Rein & Tamayo 2015) which can be downloaded freely at <http://github.com/hannorein/rebound>.

ORCID iDs

Cheng Chen  <https://orcid.org/0000-0002-4489-3491>

Rebecca G. Martin  <https://orcid.org/0000-0003-2401-7168>
 Stephen H. Lubow  <https://orcid.org/0000-0002-4636-7348>
 C. J. Nixon  <https://orcid.org/0000-0002-2137-4146>

References

- Aly, H., Dehnen, W., Nixon, C., & King, A. 2015, *MNRAS*, 449, 65
 Baran, A. S., Zola, S., Blokesz, A., Østensen, R. H., & Silvotti, R. 2015, *A&A*, 577, A146
 Barclay, T., Quintana, E. V., Raymond, S. N., & Penny, M. T. 2017, *ApJ*, 841, 86
 Bate, M. R. 2018, *MNRAS*, 475, 5618
 Bate, M. R., Bonnell, I. A., Clarke, C. J., et al. 2000, *MNRAS*, 317, 773
 Berger, T. A., Huber, D., Gaidos, E., & van Saders, J. L. 2018, *ApJ*, 866, 99
 Boss, A. P. 2011, *ApJ*, 731, 74
 Brinch, C., Jørgensen, J. K., Hogerheijde, M. R., Nelson, R. P., & Gressel, O. 2016, *ApJL*, 830, L16
 Capelo, H. L., Herbst, W., Leggett, S. K., Hamilton, C. M., & Johnson, J. A. 2012, *ApJL*, 757, L18
 Chambers, J., Wetherill, G., & Boss, A. 1996, *Icar*, 119, 261
 Chen, C., Franchini, A., Lubow, S. H., & Martin, R. G. 2019, *MNRAS*, 490, 5634
 Chen, C., Lubow, S. H., Martin, R. G., & Nixon, C. J. 2023a, *MNRAS*, 521, 5033
 Chen, C., Lubow, S. H., & Martin, R. G. 2020, *MNRAS*, 494, 4645
 Chen, C., Lubow, S. H., & Martin, R. G. 2022, *MNRAS*, 510, 351
 Chen, C., Martin, R. G., & Nixon, C. J. 2023b, *MNRAS*, 525, 3781
 Chiang, E. I., & Murray-Clay, R. A. 2004, *ApJ*, 607, 913
 Childs, Anna C., & Martin, Rebecca G. 2022, *ApJL*, 935, L31
 Clanton, C., & Gaudi, B. S. 2017, *ApJ*, 834, 46
 Clarke, C. J., & Pringle, J. E. 1993, *MNRAS*, 261, 190
 Czekala, I., Chiang, E., Andrews, S. M., et al. 2019, *ApJ*, 883, 22
 Doolin, S., & Blundell, K. M. 2011, *MNRAS*, 418, 2656
 Esmer, E. M., Baştürk, Ö., Selam, S. O., & Aliş, S. 2022, *MNRAS*, 511, 5207
 Farago, F., & Laskar, J. 2010, *MNRAS*, 401, 1189
 Fleming, D. P., Barnes, R., Graham, D. E., Luger, R., & Quinn, T. R. 2018, *ApJ*, 858, 86
 Franchini, A., Martin, R. G., & Lubow, S. H. 2020, *MNRAS*, 491, 5351
 Gladman, B. 1993, *Icar*, 106, 247
 Gong, Y.-X. 2017, *ApJ*, 834, 55
 Gong, Y.-X., & Ji, J. 2017, *AJ*, 154, 179
 Holman, M. J., & Wiegert, P. A. 1999, *AJ*, 117, 621
 Kennedy, G. M., Matrà, L., Facchini, S., et al. 2019, *NatAs*, 3, 278
 Kennedy, G. M., Wyatt, M. C., Sibthorpe, B., et al. 2012, *MNRAS*, 421, 2264
 Kenworthy, M. A., González Picos, D., Elizondo, E., et al. 2022, *A&A*, 666, A61
 Koshimoto, N., Sumi, T., Bennett, D. P., et al. 2023, *AJ*, 166, 107
 Kostov, V. B., McCullough, P. R., Hinse, T. C., et al. 2013, *ApJ*, 770, 52
 Kostov, V. B., Orosz, J. A., Feinstein, A. D., et al. 2020, *AJ*, 159, 253
 Kozai, Y. 1962, *AJ*, 67, 591
 Kratter, K. M., & Shannon, A. 2014, *MNRAS*, 437, 3727
 Lidov, M. L. 1962, *P&SS*, 9, 719
 Lubow, S. H., & Martin, R. G. 2018, *MNRAS*, 473, 3733
 Lubow, S. H., & Ogilvie, G. I. 2000, *ApJ*, 538, 326
 Ma, S., Mao, S., Ida, S., Zhu, W., & Lin, D. N. C. 2016, *MNRAS*, 461, L107
 Manara, C. F., Morbidelli, A., & Guillot, T. 2018, *A&A*, 618, L3
 Tychoniec, Ł., Manara, C. F., Rosotti, G. P., et al. 2020, *A&A*, 640, A19
 Marchal, C., & Bozis, G. 1982, *CeMec*, 26, 311
 Martin, D. V. 2019, *MNRAS*, 488, 3482
 Martin, D. V., & Fabrycky, D. C. 2021, *AJ*, 162, 84
 Martin, R. G., & Lubow, S. H. 2017, *ApJL*, 835, L28
 Martin, R. G., Lubow, S. H., Nixon, C., & Armitage, P. J. 2016, *MNRAS*, 458, 4345
 Miret-Roig, N., Bouy, H., Raymond, S. N., et al. 2021, *NatAs*, 6, 89
 Mróz, P., Udalski, A., Skowron, J., et al. 2017, *Natur*, 548, 183
 Naoz, S., Li, G., Zanardi, M., de Elía, G. C., & Di Sisto, R. P. 2017, *AJ*, 154, 18
 Nixon, C. J., Cossins, P. J., King, A. R., & Pringle, J. E. 2011, *MNRAS*, 412, 1591
 Nixon, C. J., King, A. R., & Pringle, J. E. 2018, *MNRAS*, 477, 3273
 Orosz, J. A., Welsh, W. F., Carter, J. A., et al. 2012a, *ApJ*, 758, 87
 Orosz, J. A., Welsh, W. F., Carter, J. A., et al. 2012b, *Sci*, 337, 1511
 Papaloizou, J. C. B., & Terquem, C. 1995, *MNRAS*, 274, 987
 Pflyffer, S., Alibert, Y., Benz, W., & Swoboda, D. 2015, *A&A*, 579, A37
 Quarles, B., Li, G., Kostov, V., & Haghighipour, N. 2020, *AJ*, 159, 80

- Quarles, B., Satyal, S., Kostov, V., Kaib, N., & Haghighipour, N. 2018, *ApJ*, 856, 150
- Raghavan, D., McAlister, H. A., Henry, T. J., et al. 2010, *ApJS*, 190, 1
- Rasio, F. A., & Ford, E. B. 1996, *Sci*, 274, 954
- Rein, H., & Liu, S. F. 2012, *A&A*, 537, A128
- Rein, H., & Tamayo, D. 2015, *MNRAS*, 452, 376
- Reipurth, B., & Clarke, C. 2001, *AJ*, 122, 432
- Smullen, R. A., Kratter, K. M., & Shannon, A. 2016, *MNRAS*, 461, 1288
- Standing, M. R., Sairam, L., Martin, D. V., et al. 2023, *NatAs*, 7, 702
- Sumi, T., Kamiya, K., Bennett, D. P., et al. 2011, *Natur*, 473, 349
- Sumi, T., Koshimoto, N., Bennett, D. P., et al. 2023, *AJ*, 166, 108
- Sutherland, A. P., & Fabrycky, D. C. 2016, *ApJ*, 818, 6
- Thompson, S. E., Coughlin, J. L., Hoffman, K., et al. 2018, *ApJS*, 235, 38
- Turrini, D., Zinzi, A., & Belinchon, J. A. 2020, *A&A*, 636, A53
- Veras, D., & Raymond, S. N. 2012, *MNRAS*, 421, L117
- Verrier, P. E., & Evans, N. W. 2009, *MNRAS*, 394, 1721
- von Zeipel, H. 1910, *AN*, 183, 345
- Weidenschilling, S. J., & Marzari, F. 1996, *Natur*, 384, 619
- Weiss, L. M., Marcy, G. W., Petigura, E. A., et al. 2018, *AJ*, 155, 48
- Welsh, W. F., Orosz, J. A., Carter, J. A., et al. 2012, *Natur*, 481, 475
- Whitworth, A. P., & Zinnecker, H. 2004, *A&A*, 427, 299
- Winn, J. N., Holman, M. J., Johnson, J. A., Stanek, K. Z., & Garnavich, P. M. 2004, *ApJL*, 603, L45
- Zanazzi, J. J., & Lai, D. 2017, *MNRAS*, 467, 1957
- Zhang, Z., & Fabrycky, D. C. 2019, *ApJ*, 879, 92
- Zhu, W., Bernhard, K., Dai, F., et al. 2022, *ApJL*, 933, L21